Modern Geology
1975, Vol. 5, pp. 155-164

TEMPERATURE GRADIENTS IN METEORITES PRODUCED BY HEATING DURING ATMOSPHERIC PASSAGE

D. W. SEARS†

Departments of Astronomy and Geology, University of Leicester, Leicester, England.

Presented by M. J. Aitken

Abstract—The extent to which high temperatures experienced by the surface of the meteorite during its atmospheric passage have penetrated into the meteorite may be determined by fusion crust and thermoluminescence (*TL*) methods. The *TL* results suggest luminous flight times in the order of 10 seconds, but the gradients tend to be 3–5 times less than those predicted theoretically. They appear to have the same dependence on the orientation of the meteorite as the temperature gradients determined from the fusion crust; the steepest gradients being experienced at the front of the meteorite. The fusion crust, besides enabling much of the atmospheric behaviour to be determined, provides a useful source of information complementary to *TL* work. For example, *TL* gradients produced by atmospheric heating will only be found when the fusion crust contains an innermost zone.

1. INTRODUCTION

Temperature gradients are produced in a meteorite by heating during its atmospheric passage. The methods so far published for their measurement are broadly of two kinds. They are either petrographic, in which changes in structure and mineralogy resulting from elevated temperatures are used; or they involve the use of thermoluminescence, *TL*. (*TL* is the light emitted when electrons drop to the valence band from the conduction band via a luminescent centre after being thermally stimulated from "traps" in the crystal lattice.) It is necessary with the petrographic methods to use a semi-theoretical approach since the gradient is not varying linearly, but approximately exponentially. The observations that have been used tend to be metallurgical, because of the greater sensitivity of iron meteorite structures to the range of temperatures involved (Buchwald, 1961; 1967; Reed, 1972; Lovering *et al.*, 1960; and Marringer and Manning, 1960). Some observations for stony meteorites were made by Clarke *et al.* (1971).

Temperature gradients are a useful complement to morphological studies since they reflect the orientation of the specimen; steeper gradients being experienced at the front of the stone. They also give a clue to the luminous flight time. Prachyabrued *et al.* (1971) employed their results in this way, while Vaz (1972) used the similarity in the temperature profiles of Lost City and Ucera to infer similar luminous flight times. In the work described in this paper the reduction in thermoluminescence near the fusion crust has been examined in several meteorites. These results are compared with those obtained from an examination of the fusion crust and also with predictions from theoretical studies.

2. METHODS

Ramdohr (1967) has pointed out a number of mineralogical changes which occur in the fusion crust. These were discussed by Sears and Mills (1973) and led to the temperature gradient determinations shown in Table I. The gradients could be measured roughly by eye directly from the curves of temperature vs. depth, but since these curves vary non-linearly this is impossible to do with any degree of consistency. Instead one may rearrange the ablation rate equation (see below) and differentiate it to show that

$$\frac{\partial T}{\partial y} = \frac{v_w T_i}{k} \exp\left(\frac{-y\, v_w}{k}\right)$$

where v_w is the ablation rate, k the thermal diffusivity (K/DC_p, where K is thermal conductivity, D is density and C_p is specific heat), T is the temperature at depth y and T_i, the surface temperature. The temperature gradient can therefore be readily calculated at any point for which the temperature and distance are known once the ablation rate has been calculated from the ablation rate equation. The fusion crust provides the data required at each step.

The alternative method of temperature gradient determination involves the measurement of thermoluminescence at various depths below the fusion

† Present address: Department of Metallurgy, The University, Manchester, England.

TABLE I
Temperature Gradients and Ablation Rates for the Barwell Meteorite

Specimen	Face Type	Temperature gradient (°C/μm)[a]	Ablation rate (cm/sec)
BM 1966,59	Front, Close	12	0.35
BM 1966,65	Front Side, Close	7.6	0.27
BM 1966,57	Lateral, Striated	6.1	0.22
BM 1966,57	Rear, Warty	3.5	0.18

[a] At the depth at which nickel-iron and troilite/nickel-iron eutectics begin to flow into the meteorite matrix (Sears and Mills, 1973).

crust (Vaz, 1971). This results in a curve of *TL* vs. depth. A calibration curve may then be prepared describing the way in which *TL* drops when the sample is heated to various temperatures for a short period, and the *TL* vs. depth curve expressed as temperature vs. depth. The apparatus and the experimental techniques have been described elsewhere (Sears and Mills, 1974), but essentially consists of molybdenum filament electrically heated at 5.0± 0.05 °C/sec by an electronic control unit. The emitted light was measured with an EMI 9635B photomultiplier tube. The powder was ground, its magnetic component removed, sieved (50 μm) and 10 mg placed on a defined area of the filament. The light emitted was automatically plotted against temperature to produce the glow curve.

3. RESULTS

3.1 *The Barwell Meteorite*

A sample of the Barwell meteorite with frontal fusion crust was used in this investigation (Leicester University Geology Department acquisition number 43801). The bar taken was at an angle of about 45° to the surface of the crust and provided thirty 1 mm thick sections of about $\frac{1}{2}$ cm^2 area. Cutting was performed with a Metals Research Ltd. Microslice II diamond saw giving a 0.10 mm wide cut. The specimen was mounted for cutting with adhesive tape and elastic bands.

The natural *TL* (Figure 1) occurs in two temperature regions 200–250 °C (*LT*) and 300–370 °C (*HT*). The exact position of the peak varies, depending on the amount of overlap with adjacent peaks (Sears and Mills, 1974). The thermoluminescence of *LT* and probably also *HT*, is the result of a number of peaks and there is evidence that this is also true of lunar samples in which the *TL* is similarly caused by feldspar (Hwang, 1974; Durrani *et al.*, 1974). It is for this reason that I prefer the less precise terms *LT* and *HT*. The existence of many peaks in *LT* makes its behaviour difficult to interpret in terms of the commonly used theory of Randall and Wilkins (1945) which assumes single isolated peaks. A better approximation to this situation is obtained by measuring peak height, rather than area, since adjacent peaks add more to the width than to the height of the peak (see Figure 2 of Sears and Mills, 1974).

The results for Barwell are presented in Figure 2. Figure 2a shows the variation in the height of *LT* along the bar. The scatter is removed by expressing the height of *LT* relative to *HT* (Figure 2b) or relative to the height of *LT* after irradiation of the drained powder to a standard dose of about 50 krad (Figure 2c). The scatter is due to sample inhomogeneity, presumably variations in the feldspar content. The peak height ratio produces a curve with less scatter, but since *HT* may also vary across the specimen, could result in the gradient being slightly underestimated. This is not a serious problem here, however, since compared to *LT*, *HT* is highly insensitive to the temperatures *LT* is being used to measure, although it is just as sensitive as *LT* to sample inhomogeneity.

Having measured the drop in *TL* as the specimens approach the fusion crust, it is necessary to convert the reduction in *TL* to the temperature that is responsible for that drop. Powder from a central portion of the stone was therefore heated for five seconds at various temperatures and its glow curve was measured. The heating was performed by placing the powder on the filament of the *TL* apparatus and holding the temperature steady for the required time. The period of time chosen is clearly very important and is discussed below. A calibration curve of *TL* vs. temperature of "pre-heating" is thereby produced (Figure 3) and by converting the *y*-axis of the

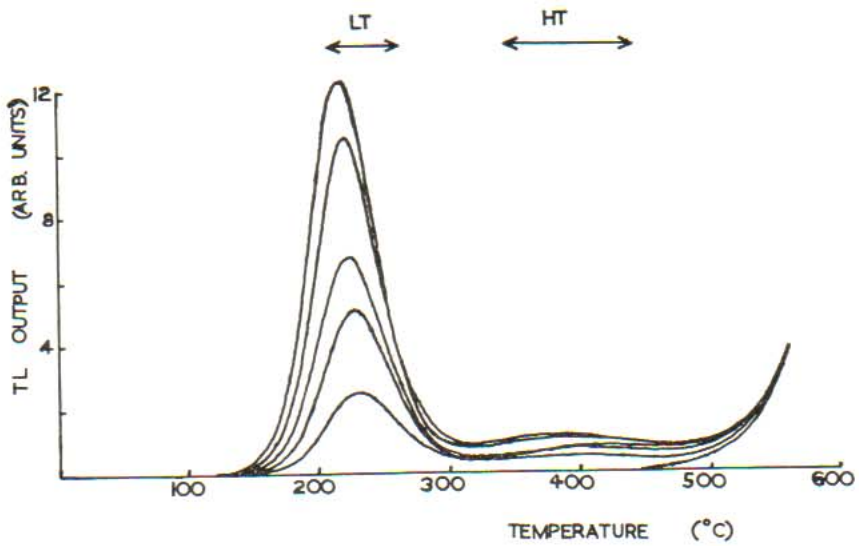

FIG. 1. Glow curves for material taken from various depths below the fusion crust of the Barwell meteorite, indicating the two regions (*LT* and *HT*) in which luminescence occurs. Note the slight movement of *LT* to higher temperatures as it drops in intensity. Variations in the height of *HT* reflect sample inhomogeneity (see Fig. 2).

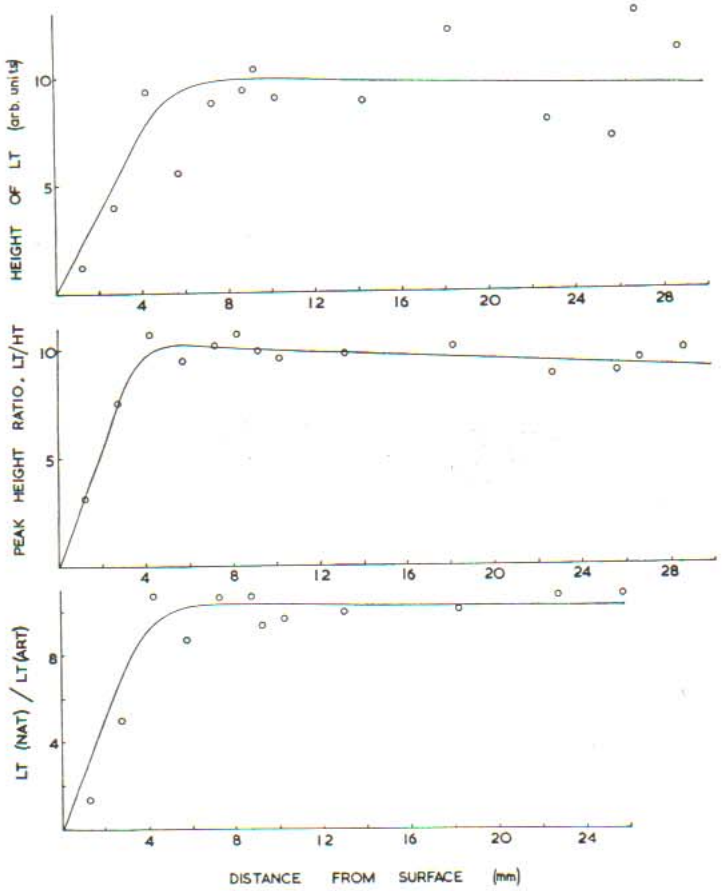

FIG. 2. Draining of the thermoluminescence by atmospheric heating near the fusion crust in a frontal specimen of the Barwell meteorite.

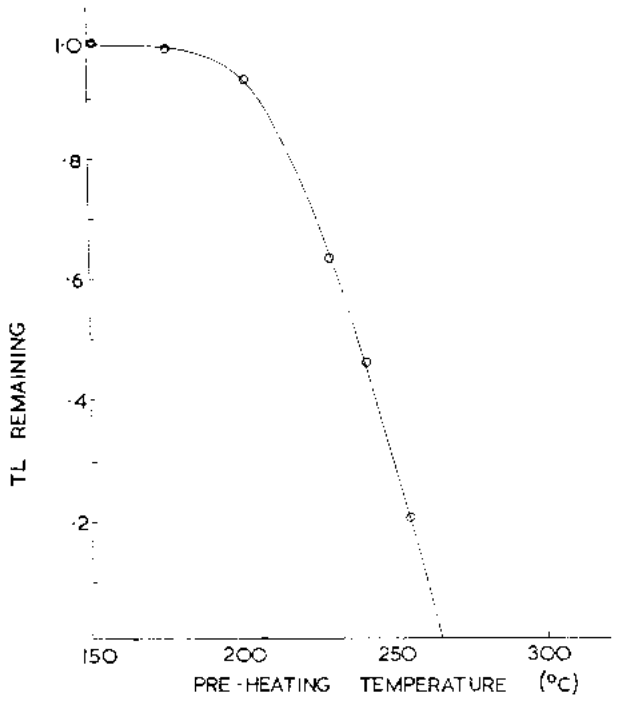

FIG. 3. The height of *LT* after the powder has been heated at various pre-heating temperatures for 5 seconds prior to measuring its *TL*. The powder was taken well from the fusion crust of the Barwell specimen.

TL vs. depth curve, and correcting for a bar normal to the surface, the temperature profile can be determined (Figure 4).

Temperatures as high as 250 °C have been experienced no further than 0.5 mm from the present surface, but temperatures exceeding 150 °C have penetrated to about 5 mm. The mean gradient at a depth exceeding 1 mm is 15–20 °C/mm.

The semi-theoretical results calculated from the fusion crust measurements are presented in Table I. Since the temperature at the troilite/troilite–nickel iron melting boundary is probably the one most reliably known it is to this boundary that the method has been applied. The results illustrate the strong dependence, at the shallow depth represented by the fusion crust, of the temperature gradient on the ablation rate. The gradients from the fusion crust and *TL* may be expected to differ because the fusion crust results apply to a depth of a few hundred micrometers, while the *TL* figures apply to depths of many millimeters and, as we shall see, the temperature drops off approximately exponentially with depth.

3.2 *The Allende Meteorite*

In a study described by Sears and Mills (1974b) several 4 × 4 mm bars were taken from a slice of an Allende stone (NMNH 3636). The bars intercepted the fusion crust at 8 locations. 1 mm thick slices were prepared from each of these bars and atmosphere-induced *TL* gradients sought. In four cases the exceptional inhomogeneity shown by Allende obscured the gradients. However, the remainder had detectable gradients and these are presented in Figure 5. The temperatures are approximate because of the uncertainty in the average value for the meteorite (possibly ±20%) but relatively the accuracy is better. The shape of the stone suggested an orientation, although not very convincingly, and the fusion crust supported this; face *d* has a temperature gradient of 5 °C/μm (for an ablation rate of 0.39 cm/sec) and face *b* a value of 4.1 °C/μm (for an ablation rate of 0.31 cm/sec). The *TL*-measured temperature gradients are in agreement with these trends and support the suggestion that *d* is the front and *b* the rear of the stone.

3.3 *The Plainview Meteorite*

Two bars were removed from an approximately rectangular 4 mm thick section of the meteorite (BM 1959,805). They intercepted the crust at four locations, at approximately 90° to each other. However, a temperature gradient could be detected by *TL* for only one of them. In section the fusion crust always shows a well developed outermost zone, but contains an innermost (FeS/NiFe–FeS eutectic flow) zone only for the surface at which *TL* could detect a temperature gradient. It appears that with the exception of this one face the stone was not exposed to heat long enough to produce temperature gradients or an innermost zone, although it was able to produce a uniform coating of fusion crust.

3.4 *The Estacado Meteorite*

Temperature gradients were sought in specimens taken from three fusion-crusted edges of a 17 kg slice of the Estacado meteorite (BM 1906,259). The meteorite was badly weathered, and only *HT* was present in the glow curves. The fusion crust specimens showed none of the characteristic features; only large bands of limonite and altered meteorite matrix were present. No *TL* gradients due to atmospheric heating could be detected in this meteorite. (The higher temperatures needed to diminish the *HT* peak would affect only the outermost millimeter or so.)

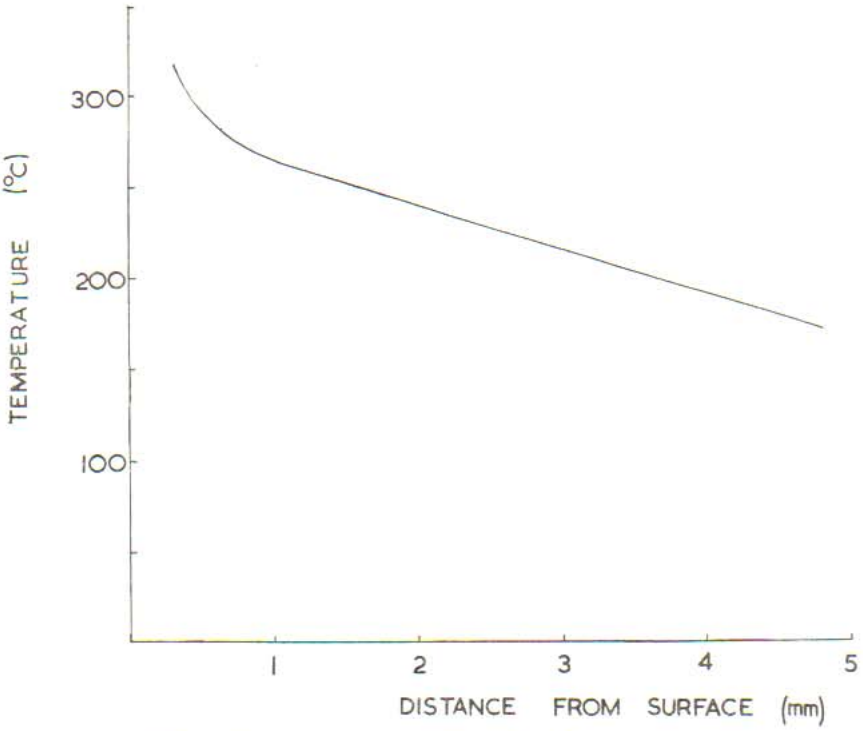

FIG. 4. The temperature profile for the Barwell meteorite.

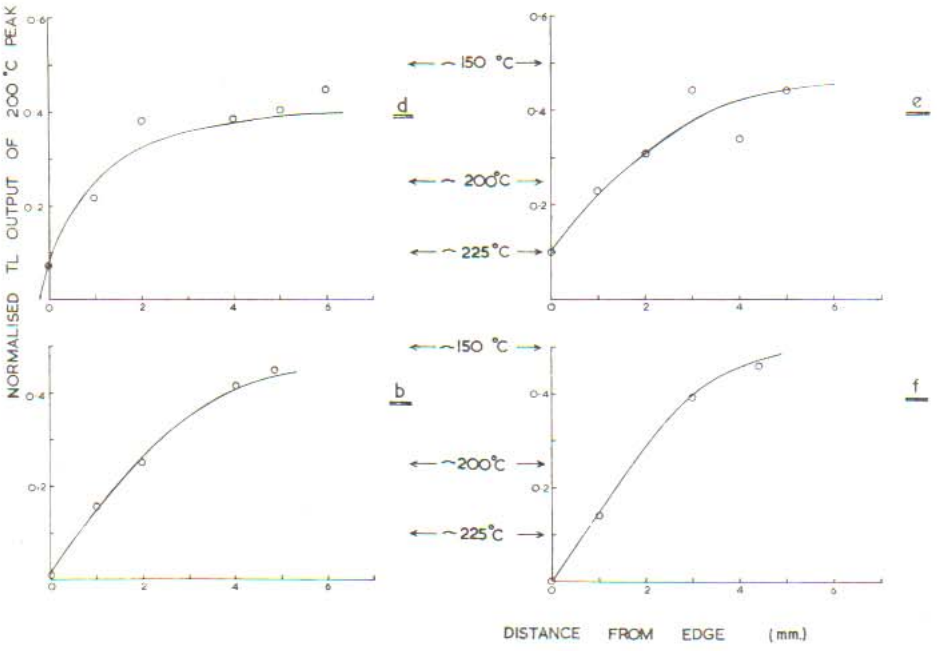

FIG. 5. The *TL* variation across a slice of the Allende meteorite showing the drop near the edge caused by atmospheric heating. Also shown are approximate temperatures thought to be required to produce that drop. The temperature gradients indicated differ in such a way as to infer that *d* is the front and *b* the rear of the stone.

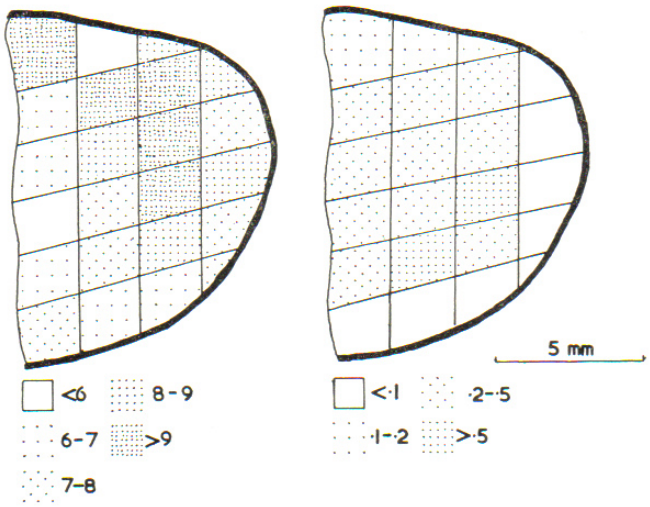

FIG. 6. The distribution of thermoluminescence across a small Holbrook stone. *a* (left) the intensity of the *TL* produced by material that has been drained and irradiated to about 300 krad. This reflects the feldspar distribution. *b* (right) the ratio of natural to artificial *TL* plotted across the slice. This describes the heat penetration. The *TL* has been considerably reduced near the primary fusion crust (heavy line) but not near the secondary crust. The *TL* intensity is in arbitrary units.

Weathering has a complicated effect on the *TL* of meteorites. Sears and Mills (1974) stated that it changes the peak height ratio, presumably by filtering the light from one peak more than the other. We also believe that the peak at about 250 °C, usually apparent as an inflexion on the low temperature side of *HT*, is due to weathering. It is only present in weathered meteorites and is more intense near the weathered crust of Estacado.

3.4 *The Holbrook Meteorite*

A 2 mm thick slice was taken from a small (5 g) completely encrusted stone (Leicester University Geology Department acquisition number 24239). The slice was too small to be cut into bars, but instead was cut into 23 2 × 2 mm squares. The distribution of the natural *TL*, and the *TL* produced by irradiating the drained powder to about 50 krad, is given in Figure 6. The natural *TL* distribution reflects the penetration of heat into the meteorite, plus the distribution of feldspar, while the artificial *TL* reflects mainly the distribution of feldspar over the slice. The flat surface of the approximately hemi-spherical slice appears not to have been exposed to heat and in the hand specimen is clearly seen to be a secondary face, whereas the rest was a primary crust. In section the secondary crust was found not to possess an innermost zone (Figure 7).

4. DISCUSSION

4.1 *Theory of Temperature Gradients and the Ablation Rates of Meteorites*

The conductivity equation, describing the temperature T at depth y, can be written to include a term for ablation in the following form:

$$\frac{\partial^2 T}{\partial y^2} + \frac{v_w}{k}\frac{\partial T}{\partial y} - \frac{1}{k}\frac{\partial T}{\partial t} = 0$$

where the symbols are as defined earlier and t is time (Carslaw and Jaeger, 1959). The solution to this is

$$T = \tfrac{1}{2}T_i\left\{\operatorname{erfc}\left(\frac{y + v_w t}{2(kt)^{1/2}}\right) + \exp\left(\frac{-v_w y}{k}\right)\operatorname{erfc} \times \left(\frac{y - v_w t}{2(kt^{1/2}}\right)\right\}$$

where

$$\operatorname{erfc} x = \frac{2}{\pi^{1/2}}\int_x^\infty \exp(-x^2)\,dx.$$

This requires considerable computation but may be simplified by considering the two cases;

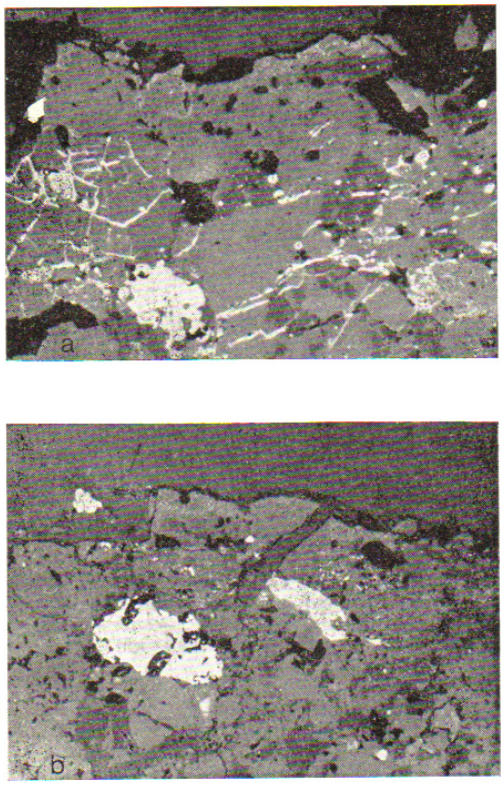

FIG. 7. Fusion crust specimens of the slice of the Holbrook meteorite shown in Figure 6, as seen in reflected light. The outer 2 mm is visible. (a) A well developed primary crust showing all three zones, (b) a secondary crust with no innermost zone.

i) Steady state conditions ($\partial T/\partial t = 0$); then the temperature distribution is

$$T = T_i \exp(-v_w y/k)$$

which is the equation applicable to the fusion crust (Bethe and Adams, 1959; Adams, 1959).

ii) Zero ablation; when a steady state is not established and the temperature distribution is governed by the time during which heat flows in. Then

$$T = T_i \operatorname{erfc}\left(\frac{y}{2(kt)^{1/2}}\right)$$

The results obtained from these two equations are shown in Figure 8, which also includes the results for iron meteorites taken from Lovering *et al.* (1960).

4.2 *The Innermost Zone of the Fusion Crust and the Existence of TL Gradients*

It is now possible to understand quantitatively why the absence of the innermost zone in the fusion crust is associated with the absence of a temperature-induced *TL* gradient. This zone takes a period in the order of one second to form (Sears and Mills, 1973). The temperature gradients calculated above show that periods considerably in excess of this, say 10 to 100 seconds, are required to produce temperature gradients in the meteorite. A useful check to make before looking for atmosphere-induced temperature gradients in meteorites with *TL* would appear to be the existence of an innermost zone in the fusion crust.

4.3 *Comparison of Theoretical and TL-observed Temperature Gradients*

The temperature profiles predicted by theory and those measured by *TL* are compared in Figure 9. Two main observations may be made. Firstly that there is good agreement between theory and experiment in the temperatures experienced at depths of 5–10 mm (about 200 °C). From this we may conclude that steady-state conditions do not apply to the regions in which the *TL* gradient is caused by atmospheric heating. Instead, the *TL* measurements infer a luminous flight time in the order of 10 seconds, since 1 second would allow a temperature of 200 °C to penetrate less than a millimeter or so, and 100 seconds would permit temperatures this high to penetrate 20 mm. However, the Allende results show that orientation, and so presumably ablation, is still a major factor in controlling the temperature gradient.

Secondly, the gradients at depths of 5–10 mm measured by *TL* are always much lower than those predicted by theory. The *TL* results are 15–20 °C/mm (Barwell), 20 °C/mm (Plainview), 15–20 °C/mm (Allende), and published values for Lost City are 25 °C/mm (Prachyabrued *et al.*, 1971), and 15 °C/mm (Vaz, 1971), The theory predicts gradients of about 70 °C/mm at these depths. This is obviously an important discrepancy to explain if the atmospheric *TL* gradients are to be completely understood. The major factors in the theoretical treatment are the thermal properties, for example a higher thermal conductivity would give a lower temperature gradient. However, the thermal conductivity would need to be greater than for pure iron in order to resolve the discrepency this way. Instead, it is necessary to examine more closely the *TL*-derived temperature gradients.

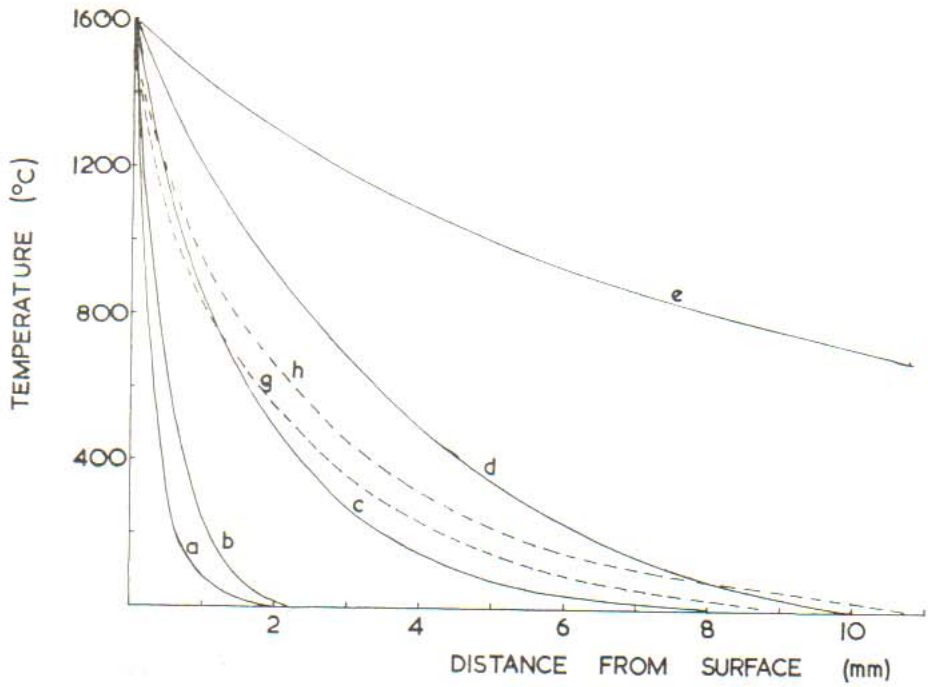

FIG. 8. Theoretical temperature gradients in meteorites. *a*, *b*, and *c* are steady-state solutions assuming ablation rates of 0.25, 0.15, and 0.05 cm/sec. *d* and *e* are non-steady-state results assuming 10 and 100 seconds luminous flight times respectively. The dotted lines are from Lovering *et al.* (1960) and are appropriate to iron meteorites; *g* is for a steady-state with an ablation rate of 0.18 cm/sec and *h* is the non-steady-state result for a 3 second luminous flight time.

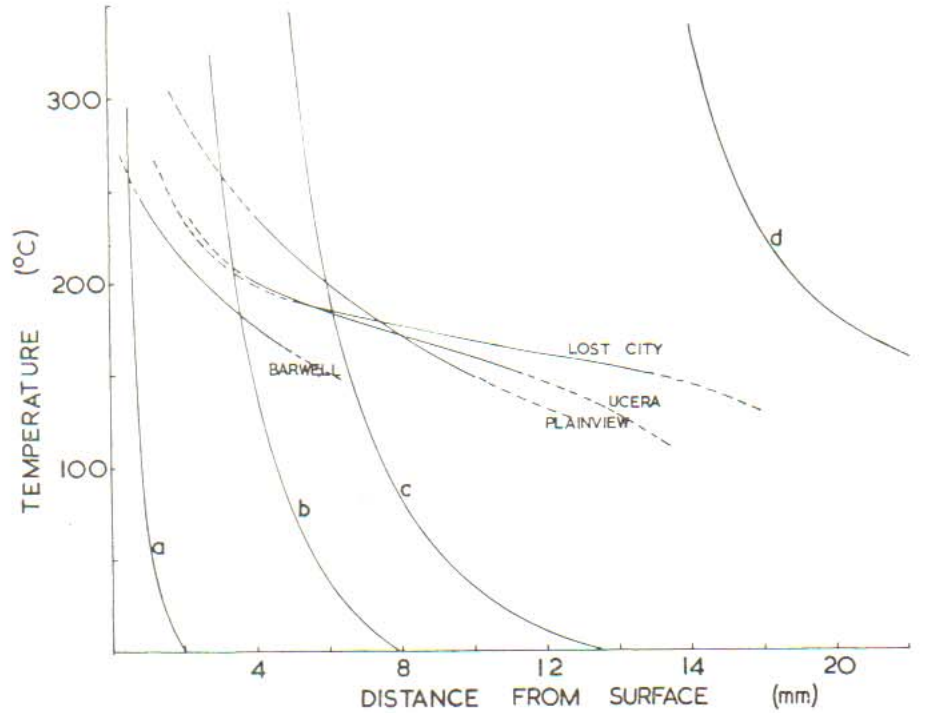

FIG. 9. A comparison of the theoretical temperature profiles with those obtained by *TL* measurement. *a* and *b* are for ablation rates of 0.25 and 0.05 cm/sec, *c* and *d* are for zero ablation for 10 and 100 second luminous flight times respectively. The *TL*-derived gradients for Lost City and Ucera are from Vaz (1971 and 1972).

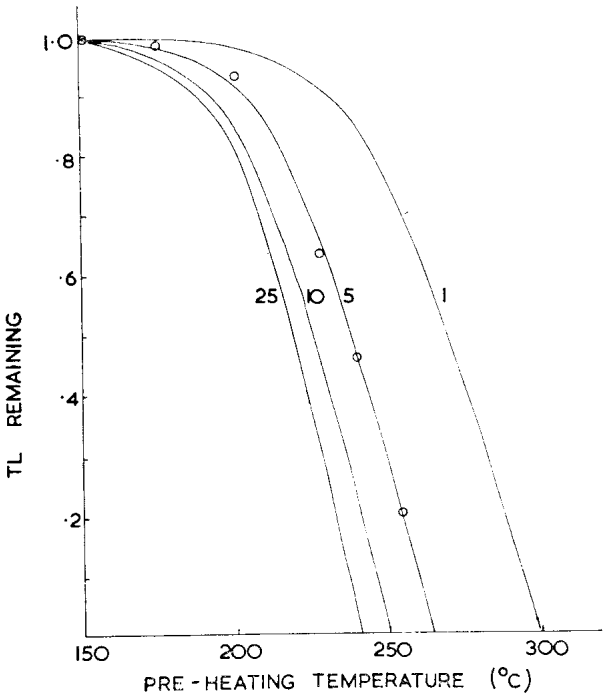

FIG. 10. The calculated height of *LT* after pre-heating to various temperatures for 1, 5, 10, and 25 seconds. The circles represent the experimental values shown in Figure 3.

4.4 *Pre-heating Curve and Pre-heating Times*

The major unknown in the *TL* procedure for measuring temperature gradients is the duration of pre-heating. This will be examined in this section. From the theory for the production of *TL* derived by Randall and Wilkins (1945) it can be readily shown that the number of trapped electrons remaining after heating for t_p seconds at a temperature of T_p is

$$n_o = n_i \exp(-st_p \exp(-E/kT_p))$$

where n_i and n_o are the number of trapped electrons before and after pre-heating, s and E are the trap parameters (the "s factor" and energy) and k is the Boltzmann constant (Garlick, 1949). Since the intensity of the *TL* is proportional to the number of excited electrons (i.e. first order decay)

$$\frac{I_p}{I} = \exp(-st_p \exp(-E/kT_p))$$

describes the proportional drop in *TL* intensity after pre-heating. s is about 10^{11} sec^{-1} (Prachyabrued *et al.*, 1971) and E is about 1.2 eV (Sears and Mills, 1974a) so that the drop in *TL* vs. pre-heating temperature may be calculated (Figure 10). The agreement

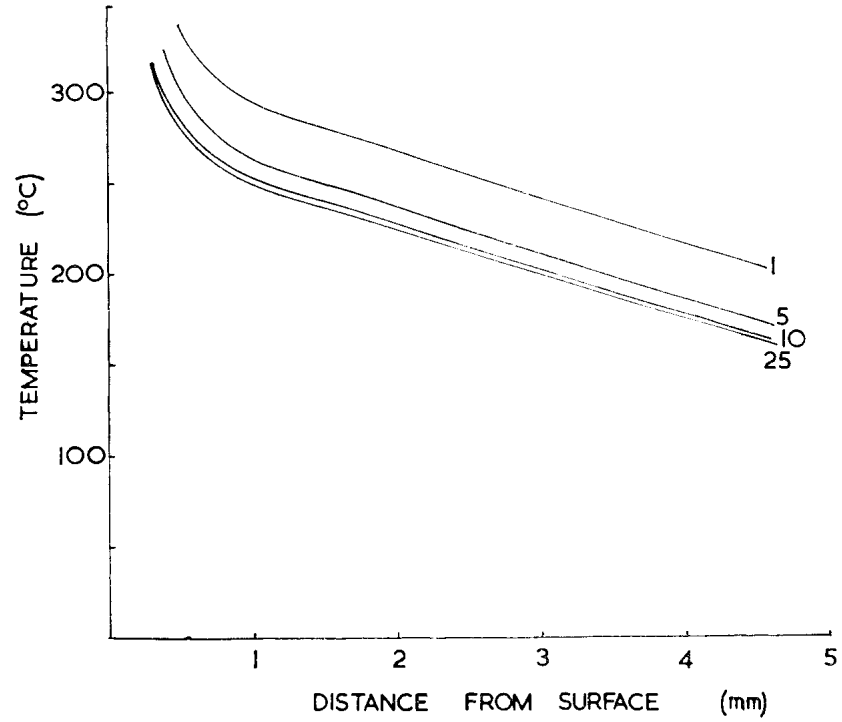

FIG. 11. Temperature profiles for the Barwell meteorite assuming various luminous flight times (and the theoretical calibration curves in Figure 10). Using different times changes the range of the temperatures concerned but does not change the gradient.

with the experimental results is excellent, and lends support to the theory and the E and s values used. The need to know the pre-heating time is also emphasised by this figure. The pre-heating time for the meteorite is probably very similar to the luminous flight time.

A short luminous flight time would therefore increase the temperatures that the *TL* would appear to be measuring. However it would not change the value of the *TL*-derived temperature gradients but merely displace them vertically (Figure 11), because the slopes of the preheating curves are similar for all values of t_p.

The explanation for the difference between the theoretical and observed temperatures gradient would appear to lie elsewhere in the experimental procedure, possibly with the finite thickness of the specimens cut from the bar.

5. CONCLUSIONS

Although in detail there are worrying discrepancies between the theoretical temperature gradients and those measured by *TL*, in broad terms there is a measure of agreement. Temperatures in the order of 200 °C have usually penetrated no further than 5–10 mm, which is consistent with a luminous flight time of the order of 10 seconds. Orientation is an important factor in determining these gradients, and they may therefore be used to complement morphological and fusion crust studies. Since the production of an innermost zone in the fusion crust takes a shorter time than a measurable temperature gradient, the existence of the former is a prerequisite to the existence of the latter. This may be used as a check prior to *TL* measurement.

I am grateful to Dr. A. A. Mills for his help with the experimental aspects of this work and to Dr. R. Hutchison (British Museum, Natural History) and Dr. R. S. Clarke (National Museum of Natural History, Washington) for supplying the meteorite specimens.

REFERENCES

Adams M. C. 1959. Recent advances in ablation. *Amer. Rocket. Soc. Jour.* Sept., 625–632.

Bethe H. and Adams M. C. 1959. Theory for the ablation of glassy materials. *Jour. Aero/Space Sci.* **26**, 321–328, 350.

Buchwald V. 1961. The iron meteorite "Thule", North Greenland. *Geochim. Cosmochim. Acta*, **25**, 95–98.

Buchwald V. F. 1967. The iron meteorite Föllinge, Sweden. *Geochim. Cosmochim. Acta*, **31**, 1559–1567.

Carslaw H. S. and Jaeger J. C. 1959. *Conduction of Heat in Solids*. Clarendon Press (Oxford).

Clark R. S., Jarosewich E., Mason B., Nelen J., Gomez M., and Hyde J. R. 1970. The Allende, Mexico, meteorite shower. *Smithsonian Contrib. Earth Science* 5.

Durrani S. A., Prachyabrued W., Cristodoulides C., Fremlin J. H., Edgington J. A., Chen R., and Blair I. M. 1972. Thermoluminescence of Apollo 12 samples: Implications for lunar temperature and radiation histories. *Proc. 3rd Lunar Sci. Conf.*, **3**, 2955–2970.

Garlick G. F. J. 1949. *Luminescent Materials*. Clarendon Press.

Hwang F. S. W. 1973. Fading of thermoluminescence induced in lunar fines. *Nature* **245**, 41–43.

Lovering J. F., Parry L. G., and Jaeger J. C. 1960. Temperatures and mass losses in iron meteorites during ablation in the earth's atmosphere. *Geochim. Cosmochim. Acta.* **19**, 156–167.

Maringer P. E. and Manning G. K. 1960. Aerodynamic heating of the Grant meteorite. *Geochim. Cosmochim. Acta*. **18**, 157–161.

Prachyabrued W., Durrani S. A., and Fremlin J. H. 1971. Thermoluminescence of the Lost City meteorite. *Meteoritics* **6**, 300–301 (Abstract only).

Ramdohr P. 1967. Die schmelzkruste der meteoriten. *Earth Planet. Sci. Letters* **2**, 197–209.

Randall J. T. and Wilkins M. F. H. 1945. Phosphorescence and electron traps. *Proc. Roy. Soc. (London) A*, **184**, 366–407.

Reed S. J. 1972. The Oktibbeha County iron meteorite. *Min. Mag.*, **38**, 623–626.

Sears D. W. and Mills A. A. 1973. Temperature gradients and atmospheric ablation rates for the Barwell meteorite. *Nature Physical Science* **242**, 25–26.

Sears D. W. and Mills A. A. 1974a. Thermoluminescence and the terrestrial age of meteorites. *Meteoritics* **9**, 47–67.

Sears D. W. and Mills A. A. 1974b. Thermoluminescence studies of the Allende meteorite. *Earth Planet. Sci. Letters* **22**, 391–396.

Vaz J. E. 1971b. Lost City meteorite: Determination of the temperature gradient induced by atmospheric friction using thermoluminescence. *Meteoritics* **6**, 207–216.

Vaz J. E. 1972. Ucera meteorite: Determination of differential atmospheric heating using its natural thermoluminescence. *Meteoritics* **7**, 77–86.